The ISME Journal (2013) 7, 2349–2360

www.nature.com/ismej

ORIGINAL ARTICLE

Sulfur oxidizers dominate carbon fixation at a biogeochemical hot spot in the dark ocean

Timothy E Mattes[1], Brook L Nunn[2], Katharine T Marshall[3], Giora Proskurowski[3], Deborah S Kelley[3], Orest E Kawka[3], David R Goodlett[4], Dennis A Hansell[5] and Robert M Morris[3]

[1]*Department of Civil and Environmental Engineering, University of Iowa, Iowa City, IA, USA;* [2]*Department of Medicinal Chemistry, University of Washington, Seattle, WA, USA;* [3]*School of Oceanography, University of Washington, Seattle, WA, USA;* [4]*Department of Pharmaceutical Sciences, University of Maryland School of Pharmacy, Baltimore, MD, USA and* [5]*Rosenstiel School of Marine and Atmospheric Science, University of Miami, Miami, FL, USA*

Bacteria and archaea in the dark ocean (>200 m) comprise 0.3–1.3 billion tons of actively cycled marine carbon. Many of these microorganisms have the genetic potential to fix inorganic carbon (autotrophs) or assimilate single-carbon compounds (methylotrophs). We identified the functions of autotrophic and methylotrophic microorganisms in a vent plume at Axial Seamount, where hydrothermal activity provides a biogeochemical hot spot for carbon fixation in the dark ocean. Free-living members of the SUP05/Arctic96BD-19 clade of marine gamma-proteobacterial sulfur oxidizers (GSOs) are distributed throughout the northeastern Pacific Ocean and dominated hydrothermal plume waters at Axial Seamount. Marine GSOs expressed proteins for sulfur oxidation (adenosine phosphosulfate reductase, sox (sulfur oxidizing system), dissimilatory sulfite reductase and ATP sulfurylase), carbon fixation (ribulose-1,5-bisphosphate carboxylase oxygenase (RuBisCO)), aerobic respiration (cytochrome *c* oxidase) and nitrogen regulation (PII). Methylotrophs and iron oxidizers were also active in plume waters and expressed key proteins for methane oxidation and inorganic carbon fixation (particulate methane monooxygenase/methanol dehydrogenase and RuBisCO, respectively). Proteomic data suggest that free-living sulfur oxidizers and methylotrophs are among the dominant primary producers in vent plume waters in the northeastern Pacific Ocean.
The ISME Journal (2013) **7,** 2349–2360; doi:10.1038/ismej.2013.113; published online 11 July 2013
Subject Category: Microbial ecology and functional diversity of natural habitats
Keywords: Axial; hydrothermal; proteomics; bacteria; SUP05; Arctic96BD-19; methylotroph

Introduction

Recent genomic studies demonstrate that many of the 6.5×10^{28} bacteria that inhabit the dark ocean (>200 m) have the genetic potential to fix carbon (Reinthaler *et al.*, 2010; Swan *et al.*, 2011). These include autotrophic and methylotrophic bacteria that have genes to fix inorganic carbon and assimilate single-carbon compounds, respectively. Hydrothermal vents are characterized by steep physical and chemical gradients that are established as hot fluids from the deep subsurface mix with cold oxidized seawater. The stable neutrally buoyant plumes that form above hydrothermal vents contain approximately 0.01% vent fluid (Lupton *et al.*, 1985) and are enriched in sulfides, iron, manganese, methane (CH_4), hydrogen (H_2) and other reduced compounds relative to background seawater (Lilley *et al.*, 1995). This steady supply of chemical energy has the potential to fuel autotrophic and methylotrophic activities in the dark ocean.

Vent-associated microbial communities are commonly dominated by bacteria (especially, alpha-, gamma- and epsilon-proteobacteria) that likely participate in the oxidation of reduced sulfur compounds, ammonia, iron, manganese, CH_4 and H_2 (Huber *et al.*, 2003, 2006, 2007; Opatkiewicz *et al.*, 2009; Dick and Tebo, 2010; Sylvan *et al.*, 2012). Members of the SUP05/Arctic96BD-19 clade of marine gamma-proteobacterial sulfur oxidizers (GSOs) are among the dominant groups identified at venting locations (Sunamura *et al.*, 2004; Anantharaman *et al.*, 2013; Anderson *et al.*, 2013). Marine GSOs were first identified in the tissues of clams and mussels living at hydrothermal vents and cold seeps (Cavanaugh *et al.*, 1987; Distel *et al.*, 1988). Members of this group are closely related to thiotrophic bacteria that obtain energy from the

Correspondence: RM Morris, School of Oceanography, University of Washington, Seattle, WA 98195, USA.
E-mail: morrisrm@uw.edu
Received 8 March 2013; revised 25 May 2013; accepted 31 May 2013; published online 11 July 2013

oxidation of reduced sulfur compounds (Distel *et al.*, 1988). Similar to other symbiotic relationships in sulfide-rich marine ecosystems, the host provides access to reduced sulfur sources for autotrophic bacteria and the bacterial symbionts provide the host with a source of organic carbon (Childress *et al.*, 1991; Robinson and Cavanaugh, 1995).

Abundant and free-living marine GSOs have recently been identified in diverse seawater samples (Lavik *et al.*, 2009; Walsh *et al.*, 2009; Swan *et al.*, 2011). Marine GSOs accounted for 45% of the 16*S* ribosomal RNA (rRNA) gene clones recovered from an oxygen-minimum zone in the South Atlantic and 37% of the bacterial 16*S* rRNA genes recovered from an anoxic fjord in British Columbia (Lavik *et al.*, 2009; Walsh *et al.*, 2009). Marine GSOs dominated bacterial communities (88–90%) in the plume layer in the Suiyo Seamount caldera (Sunamura *et al.*, 2004) and were among the key groups identified in diffuse-flow hydrothermal vent fluids in 1998–2000 following an eruption at Axial volcano in 1998 (Huber *et al.*, 2006). Recent studies have indicated that marine GSOs are abundant and active in the Guaymas Basin in the Gulf of California (Lesniewski *et al.*, 2012; Anantharaman *et al.*, 2013).

We used a tandem mass spectrometry (MS/MS)-based proteomics approach to identify expressed proteins in hydrothermal plume waters at Axial Seamount, an active volcano along the Juan de Fuca Ridge spreading center (Caress *et al.*, 2012; Chadwick *et al.*, 2012; Dziak *et al.*, 2012). We also compared microbial communities in plumes with microbial communities in other areas of the northeastern Pacific Ocean not influenced by hydrothermal systems. Our results suggest that chemolithoautotrophic marine GSOs were the dominant primary producers in hydrothermal plume fluids, with methanotrophic and iron-oxidizing bacteria contributing to a lesser extent. These data support previous findings, which combined suggest that this ubiquitous group of free-living marine GSOs are active in diverse deep ocean environments (Swan *et al.*, 2011; Anantharaman *et al.*, 2013; Lesniewski *et al.*, 2012).

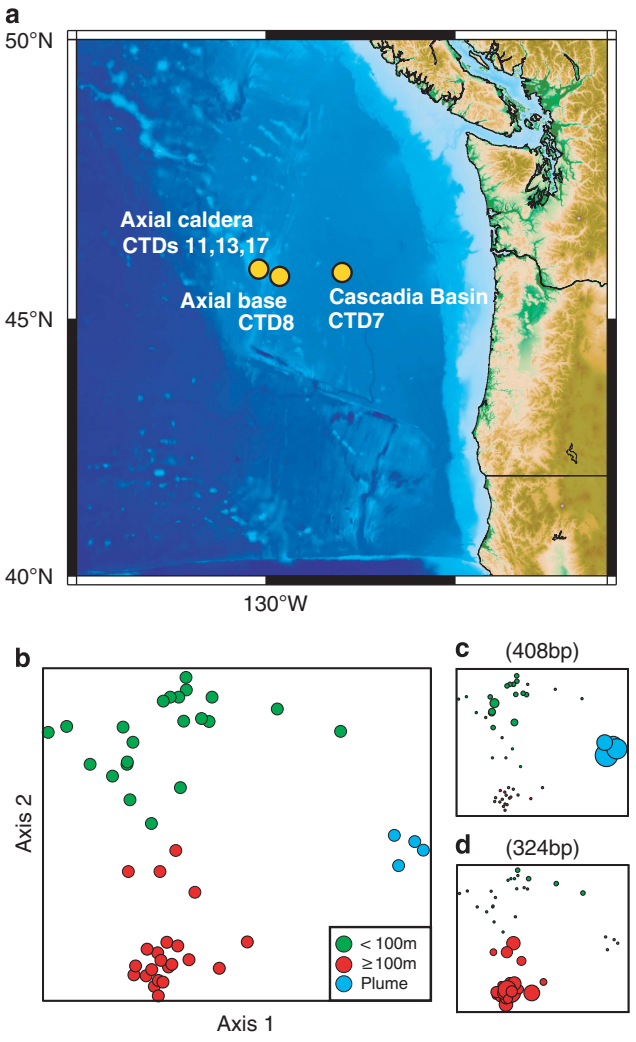

Figure 1 Station locations and NMS ordination analysis of microbial communities in the northeastern Pacific Ocean. (**a**) Stations were located in the Cascadia Basin (CTD7) and at Axial Seamount (CTD8, 11, 13 and 17). (**b**) NMS analyses of bacterial communities determined by TRFLP analyses. (**c**) NMS ordination depicting the relative abundance of a 408-bp TRF that dominated samples collected from a hydrothermal vent plume. (**d**) NMS ordination illustrating the relative abundance of a 324-bp TRF that was ubiquitous in samples collected at depths ⩾100 m. Sample sizes in panels **c** and **d** indicate relative abundance.

Materials and methods

Sample collection

All samples were collected onboard the *R/V Thomas G Thompson* during a University of Washington-led research cruise in support of the National Science Foundation's Ocean Observatory Initiative—Regional Scale Nodes cruise (19 August to 1 September 2011) from Seattle, WA, to Hydrate Ridge and Axial Seamount (Figure 1). Water samples for microbial and chemical analyses were collected using a conductivity, temperature and depth (CTD) rosette profiler equipped with 12 l Niskin bottles. Samples were collected from five different stations (CTD7 Cascadia Basin (lat: 45.8602/lon: −127.9353), CTD8 base of Axial Seamount (lat: 45.8202/lon: −129.7567), CTD11 ASHES vent field (lat: 45.9339/lon: −130.0136), CTD13 Coquille vent (lat: 45.9264/lon: −129.9803) and CTD17 ASHES vent field (lat: 45.9340/lon: −130.0138)). Sample numbers, depths and types of analyses are shown in Supplementary Table 1.

Contextual data and site description

Partial and full water column profile measurements were conducted using a rosette-mounted instrument package that included a Seabird 9plus CTD with dual temperature and conductivity sensors, a Seabird 43 oxygen sensor (calibrated to onboard Winkler titrations) and a WET Labs C-Star transmissometer. Using the downcast profile measurements, the position and

extent of the hydrothermal plume was identified by large negative deflections in beam transmission (corresponding to the high particulate load generated from precipitating metal sulfides in the hydrothermal fluid) and subtle positive anomalies in temperature (corresponding to the heat input from high-temperature fluids), following well-established plume identification practices (Baker *et al.*, 1993). At the summit of Axial Seamount, hydrothermal plumes were 30–100 m thick, with the neutrally buoyant plume having a typical rise height of 75–200 m above the seafloor.

During the profile upcast, 12 l Niskin water sampling bottles (General Oceanics, Miami, FL, USA) were triggered at depths determined to be within the hydrothermal plume and at regular intervals in the water column above the plume. Water samples were analyzed for CH_4 and H_2 concentrations using shipboard gas chromatography. Samples were headspace extracted and inlet into a gas chromatograph (SRI Instruments, Torrance, CA, USA) configured with a helium carrier, a 30 m 5 Å mol sieve column, a 50 °C isothermal temperature program, and flame ionization and pulse discharge detectors. This method provided the sensitivity to measure the low gas concentrations of background seawater (CH_4: 0.5–1 nM, H_2: 0.1–0.5 nM). Hydrothermal fluids are enriched in both CH_4 and H_2 (Lilley *et al.*, 1982; Proskurowski *et al.*, 2008).

Nutrients, dissolved organic carbon and total dissolved nitrogen

Samples for nutrient, dissolved organic carbon and total dissolved nitrogen analyses were stored frozen in 60 ml high-density polyethylene bottles until analysis within 2 months of the completion of the cruise. Nutrient concentrations were assessed by following the protocols of the WOCE Hydrographic Program using a Technicon AAII system at the University of Washington. Dissolved organic carbon and total dissolved nitrogen concentrations were assessed by high-temperature combustion using a Shimadzu TOC-csh with autoinjection (Dickson *et al.*, 2007). Four-point standard curves using potassium hydrogen phthalate and potassium nitrate were run daily to calibrate the response of the high-temperature combustion system. Measurements were quality controlled using Consensus Reference Materials distributed to the international community by the Hansell Laboratory (Hansell, 2005). The Consensus Reference Materials were analyzed at regular intervals during each analytical day. Low-carbon reference water was employed to determine system blanks. Dissolved organic nitrogen was determined as the difference in concentrations of total dissolved nitrogen and dissolved inorganic nitrogen (Supplementary Figure 1).

Microbial cell counts

Microbial cells were collected from multiple depths, fixed in filtered formalin at a final concentration of 1%, stored at 4 °C overnight and subsequently filtered (5–10 ml) onto 0.2 μm Osmonics polycarbonate filters. Total cell counts were determined by staining cells from the whole-water and concentrated seawater sample with the nucleic acid stain 4',6-diamidino-2-phenylindole (DAPI). The suite of oligonucleotide probes used to enumerate bacteria was: EUB-27R (CTGAGCCAKGATCRAACTCT), EUB-338Rpl (GCWGCCWCCCGTAGGWGT), EUB-700R (CTAHGCATTTCACYGCTACAC), EUB-700Ral (CTA CGAATTTCACCTCTACAC) and EUB-1522R (AAG GAGGTGATCCANCCVCA). The negative control oligonucleotide was 338F (TGAGGATGCCCTCCG TCG) (Morris *et al.*, 2002). Briefly, reactions were performed on membrane sections at 37 °C for 16 h in hybridization buffer (900 mM NaCl, 20 mM Tris (pH 7.4), 0.01% (w/v) sodium dodecyl sulfate and 15% or 35% formamide) and lineage-specific Cy3-labeled oligonucleotide probe suites. A control hybridization reaction was performed with a low-stringency buffer containing 15% formamide and a Cy3-labeled complementary probe (338F). Each probe had a final concentration of 2 ng μl^{-1}. Optimal hybridization stringency was achieved by hybridization washes (20 mM Tris (pH 7.4), 6 mM EDTA, 0.01% sodium dodecyl sulfate and 70 or 150 mM NaCl) for two 10-min intervals.

DAPI and fluorescence *in situ* hybridization cell counts were determined from 15 fields of view using a Nikon 80i epifluorescence microscope equipped with a Photometrics CoolSNAPHQ2 digital camera, filter sets appropriate for Cy3 and DAPI and the NIS-Elements Basic Research Acquisition and Analyses package (Nikon Instruments Inc., Melville, NY, USA). For fluorescence *in situ* hybridization, DAPI images were segmented and overlain onto corresponding Cy3 image segmentations to identify positive probe signals with corresponding DAPI signals. Negative control counts were determined using the same technique and subtracted from positive probe counts to correct for autofluorescence and nonspecific binding.

Community structural analysis

Microbial cells were collected for DNA extraction by filtering 1 liter of seawater onto sterile Supor-200 0.2 μm polyethersulfone filters. Cell lysis was performed as described previously (Morris *et al.*, 2012) with the following modifications. Onboard, filters were placed in 2 ml cryovials, flash frozen in liquid nitrogen and stored at −80 °C. To initiate cell lysis, filters were thawed on ice and sliced into sections with autoclaved scissors, and then 1 ml of sucrose lysis buffer (20 mM EDTA, 400 mM NaCl, 0.75 M sucrose and 50 mM Tris–HCl, pH 8.4) and 20 μl of lysozyme (1 mg ml^{-1}) were added. The filters were incubated for 60 min at 37 °C with shaking prior to adding 20 μl proteinase K (100 μg ml^{-1}) and 200 μl sodium dodecyl sulfate (10%) and subsequently incubated for 2 h at 55 °C

with shaking and then stored at −80 °C until DNA extraction was performed.

DNA was extracted from 600 µl of cell lysate using a DNeasy Blood and Tissue kit (QIAGEN, Germantown, MD, USA) and used for Terminal Restriction Fragment Length Polymorphism (TRFLP) analysis as described previously (Morris *et al.*, 2012). DNA concentrations were estimated with the Qubit fluorometer and the Qubit dsDNA HS assay kit. PCRs for TRFLP were conducted with 1–2 ng DNA per reaction by amplifying the 16*S* rRNA gene with 5′ end-labeled phosphoramidite fluorochrome 5-carboxy-fluorescein 27F_B (5′-AGRGTTYGATY MTGGCTCAG-3′), unlabeled 519R (5′-GWATTAC CGCGGCKGCTG-3′) primers and *Taq* polymerase as described previously (Morris *et al.*, 2012). PCR products were digested overnight at 37 °C with *Hae*III. Reaction products were cleaned using columns containing hydrated superfine Sephadex G-50. The resulting terminal restriction fragments (TRFs) were resolved along with internal size standards (50–500 bp) on an ABI 3730 DNA Analyzer (Applied Biosystems Life Technologies, Carlsbad, CA, USA) located at the Fred Hutchison Cancer Research Center in Seattle, WA, USA.

TRF sizes were estimated with Peak Scanner 1.0 (Applied Biosystems). Fragment sizes were rounded to the nearest whole number, and systematic rounding errors were manually corrected. The resulting data matrix contained 48 samples (rows) and 382 unique 16*S* rRNA gene TRFs (columns). TRFs were relativized for nonmetric multidimensional scaling (NMS) analysis by dividing the area of each fragment by the total area using the software package PC-ORD (McCune and Grace, 2002). Sorenson distances were used for NMS analysis with a random starting configuration, and the resulting solution was constrained to two dimensions. The final stress for the two-dimensional solution was 14.665 with instability of 0.00454 when using 40 real-data runs. The axes were rotated to maximize orthogonality (100%). Axis 1 explained 25.7% and axis 2 explained 58.1% of the variance (both axes explained 83.8% of the variance). The null hypothesis that there was no difference between sample groupings was rejected using the multi-response permutation procedure, which evaluates groupings with real and randomized data. A chance-corrected within-group agreement statistic of 0.24 indicated within-group homogeneity, and a *P*-value of 0 indicated that observed group differences were statistically significant.

16S rRNA gene diversity

Bacterial 16*S* rRNA gene clone libraries were constructed by amplifying community 16*S* rRNA genes with bacterial primers 27F_B and 1492R (5′-GGYTACCTTGTTACGACTT-3′) as described previously (Morris *et al.*, 2012). Briefly, amplifications were performed using community genomic DNA extracted from CTD17 (1450 m) and CTD7 (2850 m), using Apex *Taq* polymerase (Genesee Scientific, San Diego, CA, USA), and under the following conditions: 35 cycles, annealing at 55 °C for 1 min, elongation at 72 °C for 2 min and denaturation at 94 °C for 30 s. Amplicons were purified and cloned using the pGEM-T-Easy vector (Promega, Madison, WI, USA) following the manufacturer's instructions. The resulting transformations were sent to High Throughput Sequencing (HTSeq.org, Seattle, WA, USA), where clones were isolated and sequenced by Sanger sequencing using the M13F (5′-TGTAAAACGACGGCCAGT-3′) and M13R (5′-CAG GAAACAGCTATGAC-3′) primers (Supplementary Table 2).

Nearly full-length 16*S* rRNA gene sequences were obtained for frequently occurring lineages by selecting and purifying a subset of clones using the Qiagen plasmid mini-prep kit (QIAGEN). Sequencing was performed using the following primer pairs by GeneWiz Inc. (La Jolla, CA, USA): M13R, 519F (5′-CAGC(A/G)GCCGCGGTAATAC-3′), 338F (5′-ACT CCTACGGGAGGCAGC-3′) and 926R (5′-CCGTC AATTC(A/C)TTT (A/G)AGTTT-3′). Sequences were assembled with the CAP3 Sequence Assembly Program (Huang and Madan, 1999) and annotated by using the Bayesian method of Wang *et al.* (2007), which contained a custom training set augmented with marine environmental clades (Iverson *et al.*, 2012), and the SILVA least common ancestor classification tool (Pruesse *et al.*, 2007). *In silico* restriction analysis and other DNA sequence manipulation operations were performed with the Sequence Manipulation Suite (Stothard, 2000). Restriction fragments were verified for a subset of clones to confirm predicted fragment sizes. Bacterial 16*S* rRNA sequences generated during this study were submitted to GenBank (accession nos. KC522839–KC522949).

Phylogenetic relationships of marine GSOs

Phylogenetic relationships were determined using a subset of published 16*S* rRNA gene sequences. A marine GSO reference tree was obtained by selecting nearly complete (>1300 bp), high-quality, nonredundant 16*S* rRNA gene sequences from public data sets ($n = 65$). Sequences were first aligned and trimmed using MUSCLE and then manually pruned to maintain tree topology. A maximum likelihood tree that contained only the highest quality set of unique sequences ($n = 50$) was constructed using RAxML. The GTRGAMMA model was used to evaluate 100 tree topologies with 1000 bootstrap analyses. Trees were visualized using FigTree and rooted with *Methylococcus capsulatus* (GenBank accession no. AJ563935).

Plume proteomics

Seawater (~180 l) was collected from the stable hydrothermal vent plume issuing from the black smoker chimney Inferno (CTD17, 1450 m). Whole

water was transferred to clean 50 l polystyrene reservoirs and concentrated to ~230 ml with a Pellicon 2 tangential flow filtration system equipped with a 30-kDa Biomax Polyethersulfone cassette (Millipore Co., Billerica, MA, USA) as described previously (Morris *et al.*, 2010). Cells were collected and concentrated in approximately 2 h. Concentrated cells were flash frozen in liquid nitrogen and stored at −80 °C until further processing at the University of Washington. Cell counts before and after filtration (6.9×10^{10} and 2.9×10^{10}, respectively) indicate that we recovered 42% of the cells present in 180 l of hydrothermal vent plume water. Cells in the concentrated sample were divided into replicate samples (Av1 and Av2, ~115 ml each) and harvested by centrifuging at 4 °C for 60 min (17 000 *g*). The supernatant was discarded, and cell pellets were rinsed with 100 μl of 20 mM Tris buffer (pH 7.4) and stored at −80 °C.

Cells were lysed using a titanium sonicating microprobe (20 s, 10 repetitions) in a 6 M urea and 50 μM ammonium bicarbonate solution. Disulfide bonds were reduced with dithiothreitol and alkylated with iodoacetic acid. After additions of ammonium bicarbonate and methanol, 2 μg of sequence grade trypsin (Promega) was added to each sample. Enzymatic digestions were incubated for 12 h at 37 °C. Resulting peptides were desalted using a macro-spin C18 column (NestGroup, Southborough, MA, USA) following the manufacturer's guidelines prior to analysis by mass spectrometry (MS).

Peptide concentrations of Axial volcano hydrothermal vent plume proteome replicates Av1 and Av2 were measured using the Thermo Scientific Nanodrop 2000/2000c, which measures the peptide bond absorbance at wavelength of 205 nm. Approximately 1 μg of peptide digest was used for each injection into the mass spectrometer. Each sample consisted of a complex mixture of peptides that was introduced into the mass spectrometer by reverse-phase chromatography using a brand new 15 cm long, 75 μm internal diameter fused silica capillary column packed with C18 particles (Magic C18AQ, 100 Å, 5 μm; Burker-Michrom Inc., Auburn, CA, USA) fitted with a 2 cm long, 100 μm internal diameter precolumn (Magic C18AQ, 200 Å, 5 μm; Michrom Bioresources Inc.). Peptides were first trapped on the precolumn (5% acetonitrile, 4 ml min^{-1}, 7 min). Chromatographic separations were performed using an acidified (formic acid, 0.1% v/v) water–acetonitrile gradient (5–35% acetonitrile in 60 min) with a total run time of 95 min.

Mass spectrometry was performed on replicates Av1 and Av2 independently using the Thermo Fisher linear ion trap–Orbitrap (LTQ-OT) hybrid tandem mass spectrometer (Thermo Fisher, San Jose, CA, USA). Peptides were analyzed using a data-independent method termed Precursor Acquisition Independent from Ion Count (PAcIFIC) (Panchaud *et al.*, 2009). Rather than requiring the mass spectrometer to select ions for fragmentation based on MS1 data, the PAcIFIC method systematically fragments ions at all m/z channels (Panchaud *et al.*, 2011). Each method file includes the full 95 min linear high-performance liquid chromatography gradient of 5–35% acetonitrile over 60 min (see above) and covers a 21.5 m z^{-1} range using 14 contiguous, unique channels that span 2.5 m z^{-1} in the mass spectrometer. This results in a total of 45 method files per PAcIFIC analytical cycle to cover a full m/z range of 400–1400.

Protein identifications

Tandem mass spectra were interrogated against a composite database containing deduced protein sequences from lineages identified in the CTD17 clone library and lineages that are dominant in the deep ocean (background seawater). The database contained marine GSOs '*Candidatus* Vesicomyosocius okutanii HA', '*Candidatus* Ruthia magnifica Cm', the SUP05 metagenome (Walsh *et al.*, 2009) and SCGC AAA001-B15 (Arctic96BD-19 draft genome); the methylotrophs *Methylobacter tundripaludum* SV96 and *Methylomicrobium alcaliphilum*; iron-oxidizing bacteria *Gallionella capsiferriformans* ES-2 and *Sideroxydans lithotrophicus* ES-1; abundant lineages in seawater '*Candidatus* Pelagibacter ubique HTCC1062' and '*Candidatus* Pelagibacter ubique HTCC1002'; ammonia-oxidizing archaea *Nitrosopumilus maritimus* SCM1, an uncultured marine group II (Iverson *et al.*, 2012); an incomplete hydrothermal vent metagenome (Xie *et al.*, 2011); and common contaminants. SEQUEST (version UW2011.01.1) was used to correlate observed tandem mass spectra to peptide sequence via theoretical tandem mass spectra from the composite database described above (Eng *et al.*, 1994, 2008). For a detailed discussion of database considerations in community proteomics, see the publication by Morris *et al.* (2010). SEQUEST parameters included a 3.75-Da peptide mass tolerance on MS1 spectra, specifying trypsin as the enzyme; variable oxidation modification on methionine (15.9949 Da) and static modification on cysteine residues (57.021464 Da) resulting from alkylation.

Results

Distribution of marine GSOs in the northeastern Pacific Ocean

TRFLP profiles from CTD 7, 8, 11 and 13 were conducted to place hydrothermal vent plume communities in a larger regional context (Figure 1a). Community structural analyses identified three distinct groupings (Figure 1b). Microbial communities in the surface layer (<100 m) were distinct from communities at depths ⩾100 m, and microbial communities directly over hydrothermal vents were distinct from those in background seawater. TRFLP profiles just above hydrothermal vents at Axial and Coquille were dominated by a 408-bp TRF, which

had the strongest positive correlation with ordination axis 1 (0.761; Table 1). The 408 bp TRF was identified as a marine GSO by constructing a 16*S* rRNA gene clone library (57 clones) from vent plume waters (CTD17, 1450 m) (Figure 1c). A different marine GSO TRF (324 bp) was observed in relatively low abundance in vent plume samples (0.1–3.2%) and at relatively high abundance in background seawater $\geqslant$100 m, where it reached 10% (Figure 1d). This fragment identity was confirmed by constructing another 16*S* rRNA gene clone library (53 clones) from 2850 m at the CTD7 station. GSO abundance was not correlated with any single environmental variable measured in this study.

Diversity of marine GSOs in the northeastern Pacific Ocean

Maximum likelihood phylogenetic analyses of nearly full-length 16*S* rRNA gene sequences indicate that marine GSOs identified in this study are closely related to marine GSOs that inhabit symbiont, open ocean, coastal and hydrothermal vent environments (Figure 2). These include sequences recovered from Saanich Inlet, the Yellow Sea, Monterey Bay, the Arabian Sea, the Benguela upwelling system, Suiyo Seamount, the Arctic and Antarctic, and the deep ocean (Bano and Hollibaugh, 2002; Fuchs *et al*., 2005; Murray and Grzymski, 2007; Kato *et al*., 2009; Lavik *et al*., 2009; Walsh *et al*., 2009; Zaikova *et al*., 2010). The Arctic96BD-19 subclade is comprised of two monophyletic lineages, including one that includes the original Arctic96BD-19 clone and the only known cultured marine GSO (Marshall and Morris, 2013).

Table 1 16*S* rRNA gene clones recovered from the Inferno hydrothermal vent plume

Taxonomic assignment	*Predicted TRF (bp)*	*Observed TRF (bp)*	*Number of clones*	*Pearson and Kendall correlations*	
				NMS axis 1	*NMS axis 2*
SUP05	193	194	1	0.220	−0.356
Gallionellaceae	221	220	2	0.496	0.006
Methylobacter sp.	255	254	2	−0.110	0.204
Methylobacter sp.	257	256	2	−0.018	−0.042
Gamma-proteobacteria	259	257	1	−0.074	0.078
SAR11	293	291	2	0.079	0.665
Methylomonas sp.	322	322	1	0.229	−0.124
SUP05/Arctic96BD-19	323	324	3	−0.085	0.329
Arctic96BD-19	327	323	1	−0.085	0.329
SAR324	406	404	3	−0.152	−0.855
SUP05	408	406	1	0.044	0.267
SUP05	410	408	28	0.761	0.143

Abbreviations: NMS, nonmetric multidimensional scaling; rRNA, ribosomal RNA; TRF, terminal restriction fragment.
Clones were sequenced, grouped by predicted TRFs and annotations and summed to determine the number of clones recovered for each lineage (total observed). Representative clones were selected for each group, amplified, restricted and matched to TRFs observed in environmental samples. TRF correlations with NMS axes 1 and 2 correspond to fragments observed in the environmental TRFLP profiles.

The SUP05 subclade is comprised of two or more lineages, including one that includes symbionts of deep-sea clams and one that includes symbionts of deep-sea mussels and free-living representatives that inhabit both open ocean and coastal environments.

Dominance of marine GSOs in plume waters

Hydrothermal vent plume waters were sampled over the Inferno vent (Figure 3a). Cell concentrations increased by 4.5-fold from 9.58×10^4 cells per ml at 750 m to an average of 4.27×10^5 cells per ml ($\pm 3.69 \times 10^4$ cells per ml) below 1445 m over the ASHES vent field (Figure 3b). A 3–4% drop in beam transmission and a less obvious positive deflection in temperature at 1340–1470 m water depth define the stable and neutrally buoyant hydrothermal plume directly over the Inferno hydrothermal vent at ASHES. Accompanying water sample measurements of CH_4 concentrations and DAPI counts clearly show the enrichment of gases and cells in the plume relative to background levels. Dissolved oxygen above the Inferno plume shows an oxygen-minimum zone at 800–1100 m water depth and oxygen concentrations in the plume environment of $\sim 25\ \mu mol\ kg^{-1}$. Microbial biomass was subsequently concentrated from 180 l of water collected at the same location (CTD17, 1450 m) for 16*S* rRNA gene and MS/MS proteomic analysis of the Inferno vent plume microbial community (Supplementary Figure 2). Similar shifts in microbial cell counts, CH_4 and beam transmission were not observed at non-venting background locations (Supplementary Figure 2).

Fluorescence *in situ* hybridization, TRFLP and clone library analyses suggest that a single bacterial lineage dominated the Inferno hydrothermal vent plume (Table 1 and Supplementary Figure 3). Bacteria accounted for 94% of microbial cell counts, suggesting that archaea were a minor component of the plume community. TRFLP and clone library analyses were therefore conducted using bacteria-specific 16*S* rRNA gene primers. TRFLP analyses revealed the dominance of a 408-bp TRF (48%). A 16*S* rRNA gene clone library confirmed the identity of the bacterial lineage that produced this and other abundant fragments (Table 1). The majority of clones recovered from plume waters (62%) were marine GSOs with 193, 324, 406 and 408 bp TRFs. Most of them had a 408-bp TRF (28 clones). Five clones were closely related to methylotrophs, and two clones were closely related to known iron oxidizers (Table 1 and Supplementary Table 2).

Dominant activities identified in plume waters

We identified key proteins expressed by plume communities using an MS/MS-based proteomic approach. The presence of 16*S* rRNA gene sequences associated with marine GSOs,

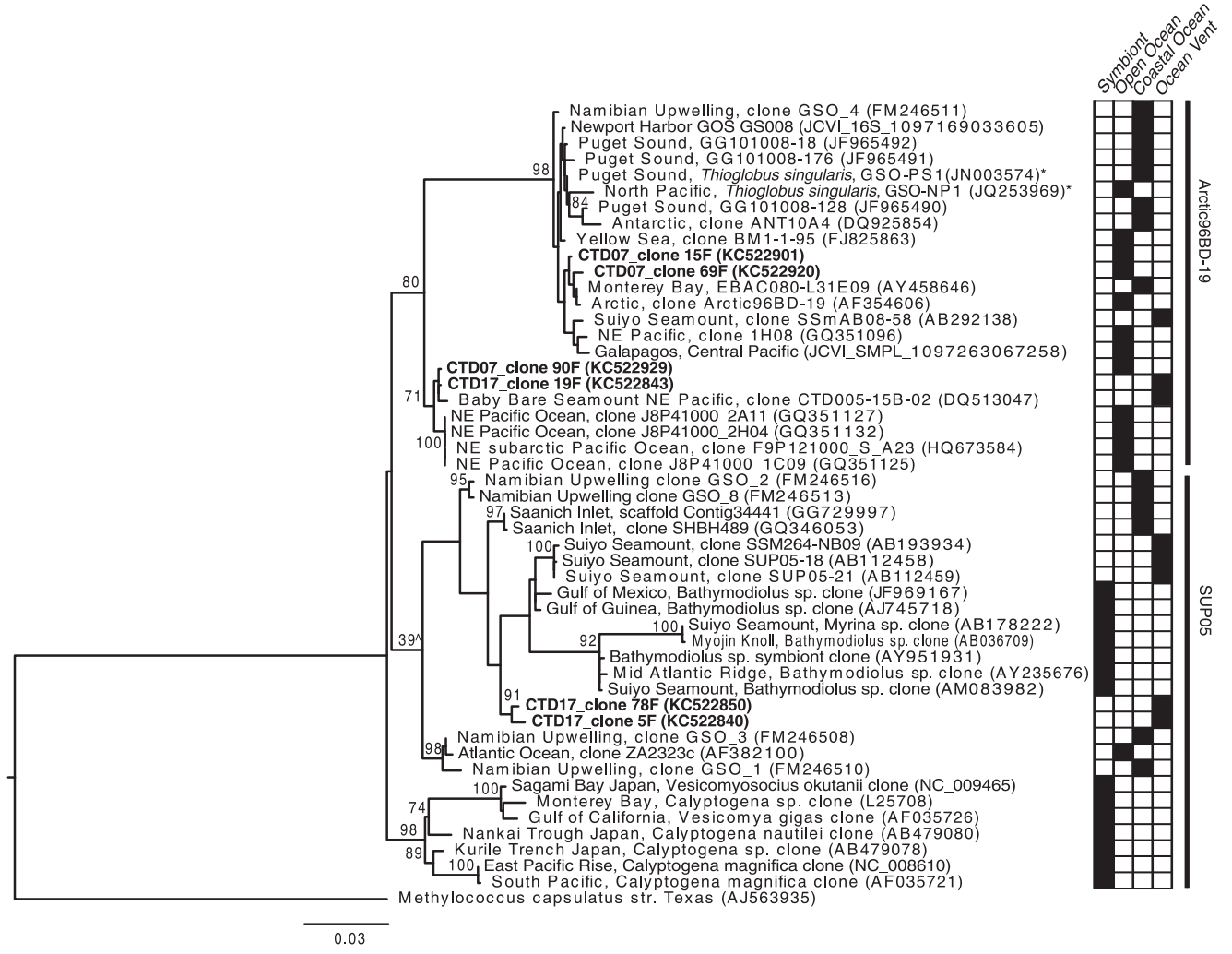

Figure 2 Phylogenetic analysis of SUP05/Arctic96BD-19 16*S* rRNA gene clones recovered from the Inferno vent plume and background seawater (1000 m). Sequences obtained in this study were aligned with those used to generate a robust maximum likelihood reference tree that contained nearly complete (1300 bp), high-quality, nonredundant reference sequences from cultures (*), environment clones and symbionts. Bootstrap values ⩾70 (1000 replicates) are reported above the nodes, except where indicated for lower values (^). *Methylococcus capsulatus* was selected as an outgroup. SUP05/Arctic96BD-19 subclade designations (black bars) are based on the study by Walsh *et al.* (2009). Symbiont and free-living (open ocean, coastal and vent) designations (right) indicate the environment from which each rRNA sequence was obtained.

methylotrophs and iron oxidizers in the CTD17 clone library informed the construction of a protein sequence database for identifying MS/MS spectra, as described in the Materials and methods section. We confidently identified 239 proteins with ⩾2 peptides in replicate Av1 (Supplementary Table 3) and 131 proteins with ⩾2 peptides in replicate Av2 (Supplementary Table 4). Although fewer proteins were identified in Av2, nearly all (94%) of the proteins identified in Av2 were also identified in Av1 (Supplementary Table 5). Differences in the total number of proteins identified in replicate samples may result from differences in the amount of biomass obtained during sample processing.

Marine GSOs, methylotrophs and iron oxidizers were active in the Inferno plume (Figure 4). Of the MS/MS spectra assigned to these lineages, 93% were from proteins expressed by marine GSOs and 5% were from proteins expressed by methanotrophs and iron oxidizers (Figure 4a). Half of the remaining 2% of MS/MS spectra were assigned to proteins expressed by members of the SAR11 clade, and half were assigned to proteins expressed by other proteobacteria (Supplementary Tables 3 and 4). A significant fraction of the marine GSO proteins (75%) were identified using a SUP05 genome sequence obtained from a Saanich Inlet metagenome. The remaining marine GSO proteins were identified using genome sequences obtained from marine GSO symbionts (Figure 4b). SUP05 proteins identified using symbiont genomes, such as cytochrome *c* oxidase (COX), are likely to be present in vent plume GSOs and symbionts but not present or not identified in GSOs from Saanich Inlet (Walsh *et al.*, 2009). COX genes were also present and expressed

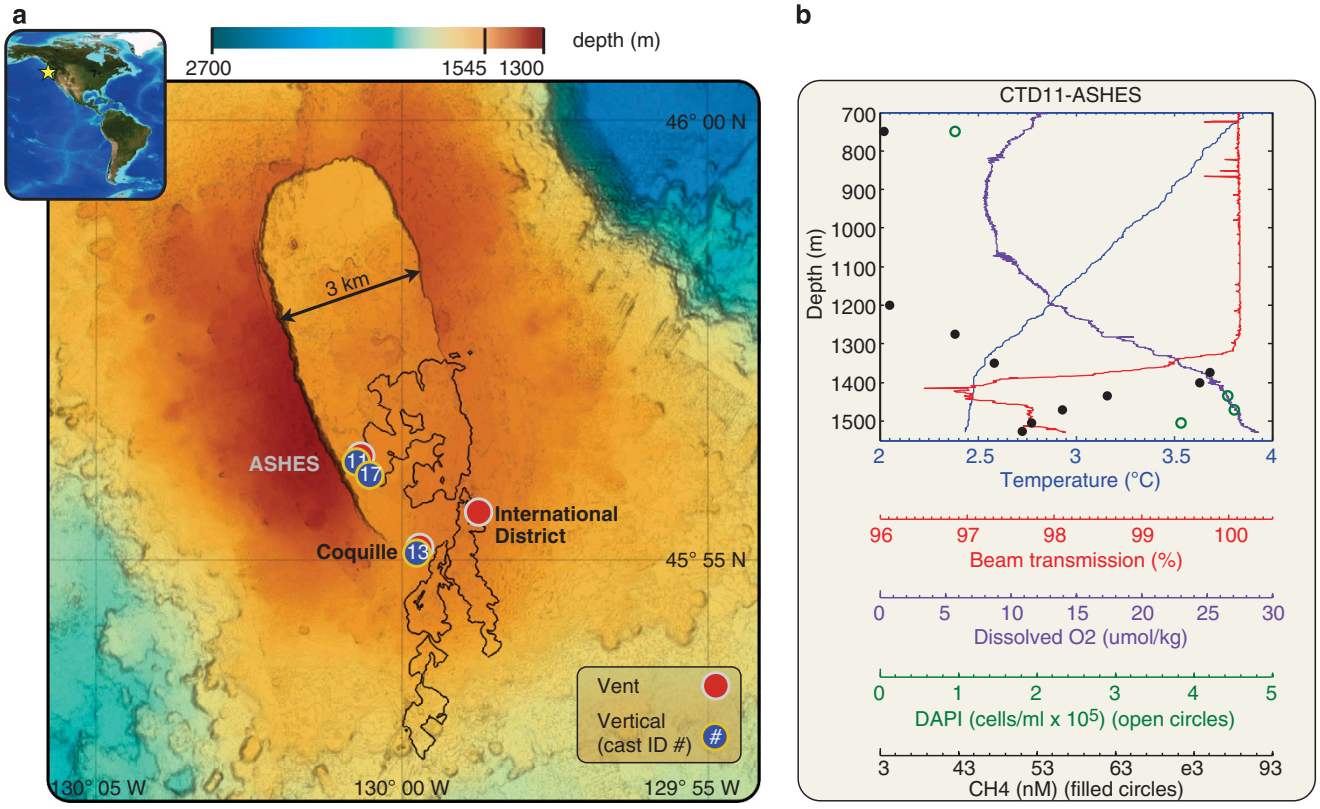

Figure 3 (**a**) Axial Seamount, located in the northeastern Pacific Ocean on the Juan de Fuca Ridge 460 km west of the Oregon coast, is influenced by hot spot and mid-ocean ridge processes. The bathymetry represents 1-m resolution mapping conducted after the 2011 eruption, and the black outline describes the boundary of the 2011 lava flows (Caress *et al*., 2012). Vertical water column profiles were conducted directly over locations of known hydrothermal venting, including nos. 11 and 17 at the ASHES hydrothermal field and no. 13 at the Coquille vent. (**b**) Vertical profile of the bottom 800 m above the ASHES vent field. A background cast was performed 215 km east of Axial Seamount at 45.9°N × 127.9°W (Supplementary Figure 2).

by SUP05 cells in hydrothermal vent plumes from the Guaymas Basin (Anantharaman *et al*., 2013).

Metabolism, genetic information processing and environmental information processing were the dominant functional classifications identified using the Kyoto Encyclopedia of Genes and Genomes. Of the MS/MS spectra assigned to these categories, 43.1% were associated with metabolism, 26% were associated with genetic information and processing and 8% were associated with environmental information processing (i.e., nitrogen regulatory protein PII) (Figure 4c). A total of 96 metabolic proteins were identified; the majority of these proteins (56.4%) were associated with energy metabolism (Figure 4d). Proteomic evidence of energy, carbohydrate, amino acid, nucleotide, vitamin and cofactor, and lipid metabolism supports the conclusion that the bacteria identified in Inferno plume waters were active.

Chemolithoautotrophy and methanotrophy in plume waters

Proteomic analysis suggests that hydrothermal vent plume marine GSOs oxidized sulfur, fixed inorganic carbon, respired oxygen and sensed nitrogen availability in plume waters. Marine GSOs and methylotrophs expressed key proteins associated with carbon fixation (Figure 5). Marine GSOs expressed proteins from several sulfur oxidation pathways, including key proteins for thiosulfate oxidation (sox), dissimilatory sulfite reductase, adenosine phosphosulfate reductase and ATP sulfurylase (SAT) (Figure 5a). Several key metabolic proteins were identified in addition to those involved in sulfur metabolism, including components of the Calvin–Benson–Basham cycle (ribulose-1,5-bisphosphate carboxylase oxygenase (RuBisCO) and a putative RuBisCO regulator), subunits I and II of COX and a nitrogen regulatory protein (PII).

The majority of methylotrophic proteins identified were associated with CH_4 and methanol oxidation (58.4% of spectra) (Figure 5b). These proteins included the β-subunit (PmoB) of particulate methane monooxygenase (pMMO), which is a characteristic of aerobic methanotrophs, and methanol dehydrogenase (XoxF). We also identified a putative methylotrophic transketolase, which could participate in formaldehyde fixation via the ribulose monophosphate pathway for carbon fixation used by some methylotrophs (Trotsenko *et al*., 1986). The formaldehyde-activating enzyme (Fae) was also

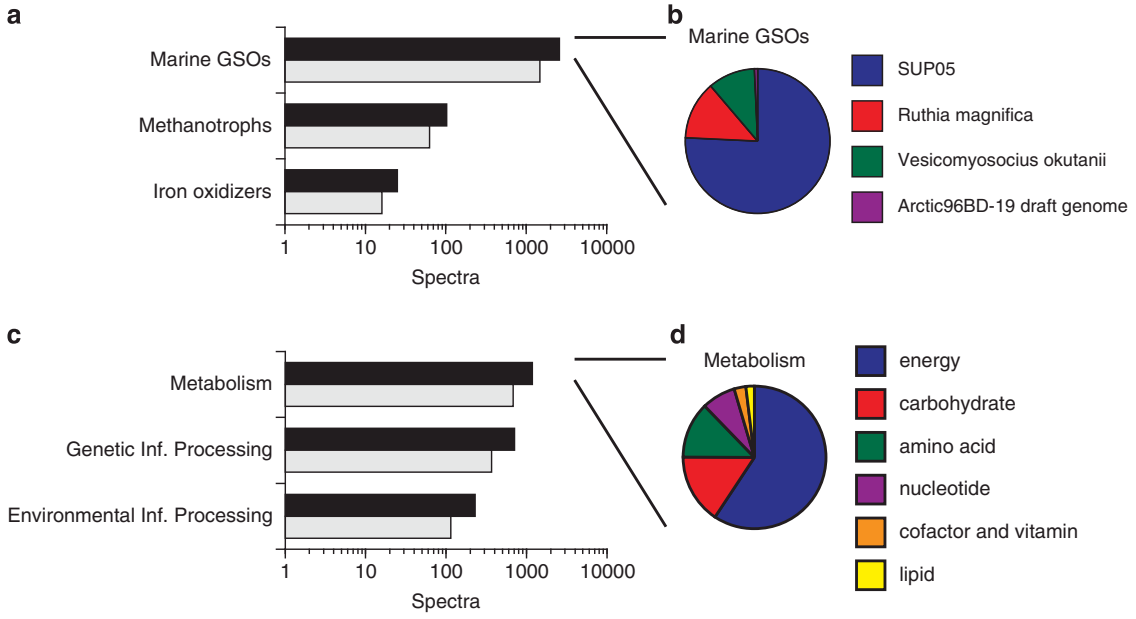

Figure 4 Dominant active bacterial groups and cellular functions expressed by bacteria and archaea in the Inferno hydrothermal vent plume. (**a**) Dominant active bacterial groups determined by consensus annotation of identified proteins, expressed in terms of total spectral counts in replicates Av1 (solid black bars) and Av2 (shaded gray bars). (**b**) Breakdown of GSO consensus protein annotations. Blue: uncultured SUP05 metagenome; red: deep-sea clam symbiont *Ruthia magnifica*; green: deep-sea clam symbiont (**c**) Dominant Kyoto Encyclopedia of Genes and Genomes categories expressed in terms of total spectral counts in replicates Av1 (solid black bars) and Av2 (shaded gray bars). (**d**) Key Kyoto Encyclopedia of Genes and Genomes metabolic functions expressed by bacteria and archaea. Relative abundance was determined by summing spectral counts for all proteins identified by two or more peptides in each category.

identified, but with lower confidence (one peptide with a protein probability of 1), which suggests that the Inferno plume harbored type I methanotrophs that assimilated carbon via the ribulose monophosphate pathway.

Discussion

These analyses suggest that free-living marine GSOs were the dominant primary producers in Inferno plume waters at Axial Seamount in 2011. Microbial community analysis suggests that members of the SUP05 subclade dominated hydrothermal plume waters at Axial volcano (ASHES and Coquille), whereas those from the Arctic96BD-19 subclade were more abundant in background seawater ($\geqslant$100 m). This suggests that vent plume communities harbor diverse marine GSOs dominated by members of the SUP05 subclade and that members of the Arctic96BD-19 subclade are more ubiquitous in the northeastern Pacific Ocean. We also identified proteins linking energy metabolism with carbon fixation, aerobic respiration and nitrogen regulation in both marine GSOs and type I methanotrophs (Figure 5).

Our findings are consistent with recent observations that marine GSOs are among the active and dominant lineages at hydrothermal vents. Marine GSOs were among the dominant lineages in plume and diffuse-flow fluids at the Main Endeavour Field and at Axial Seamount on the Juan de Fuca Ridge (Anderson *et al.*, 2013). A meta-transcriptomic study from Guaymas Basin hydrothermal plumes in the Gulf of California revealed that mRNA transcripts from ammonia oxidizers (*amoAC*), methanotrophs (*pmoABC*) and marine GSOs (*soxAY*) were greater in abundance than background seawater abundances (Lesniewski *et al.*, 2012). Methanotrophs dominated plume activities in the Guaymas Basin, whereas marine GSOs dominated plume activities at Axial volcano and ammonia oxidizers were not a significant component of the Inferno plume community. Both methodological approaches revealed the dominant lineages and key functions expressed in plumes. Differences are likely due to location and vent chemistry, as the sediment-rich Guaymas Basin provides an abundance of reduced carbon and nitrogen compounds (Lesniewski *et al.*, 2012).

Known bacterial sulfur oxidation systems fall into one of three basic groups. The first group consists of bacteria capable of complete oxidation of reduced sulfur compounds to sulfate. These organisms have a full set of sulfur oxidation genes (*sox*) including a core set (*sox*ABXYZ) and supplementary genes (*sox*CDEFGHTRSVW) (Friedrich *et al.*, 2005). A second group uses the branched thiosulfate oxidation pathway via an incomplete sox system (*sox*ABXYZ, but not *sox*C or *sox*D) and the *dsr* system (Friedrich *et al.*, 2001, 2005; Ghosh and Dam, 2009). Once the more reduced sulfur compounds have been exhausted, this group stores elemental sulfur in globules for later oxidation to sulfite by *dsr* proteins (e.g., sulfite reductase) and to sulfate by

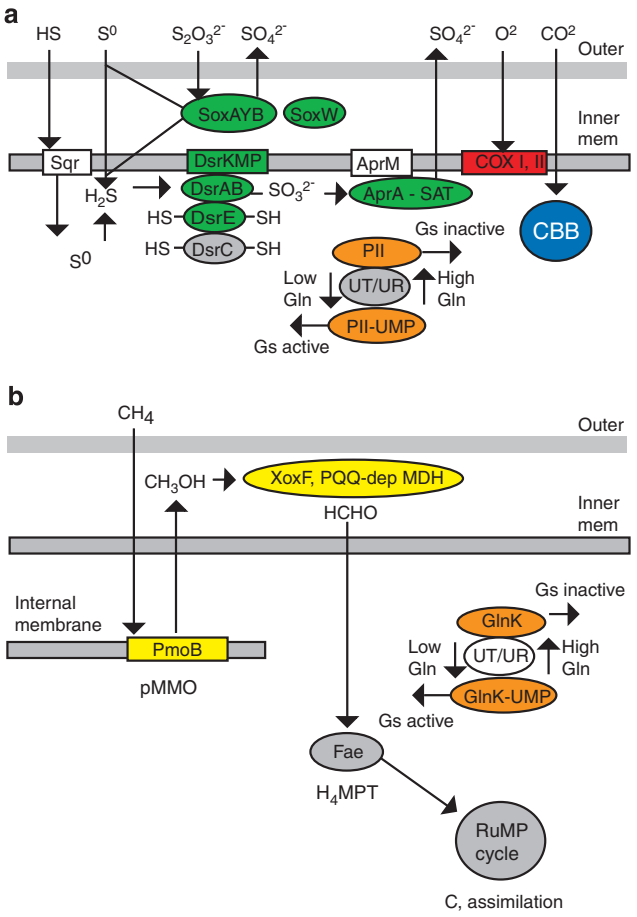

Figure 5 Illustration of sulfur oxidation and methanotrophic proteins expressed by bacteria in the Inferno hydrothermal vent plume. (**a**) Sulfur oxidation proteins expressed in the plume are indicated in green, regulatory proteins in orange, aerobic respiratory proteins in red and carbon fixation proteins in blue. (**b**) Methane oxidation proteins expressed in the plume are indicated in yellow and regulatory proteins in orange. Proteins identified by one peptide are in gray. Dsr, dissimilatory sulfite reductase; sox, sulfur oxidation system; PII, nitrogen regulatory protein PII; COX, cytochrome *c* oxidase; CBB, Calvin–Benson–Basham cycle; pMMO, particulate methane monooxygenase (PmoB); PQQ-dep MDH, PQQ-dependent methanol dehydrogenase; GlnK, nitrogen regulatory protein (homolog of PII); Gs, glutamine synthetase; UT/UR, uridylyl transferase/uridylyl-removing enzyme; Apr, adenosine phosphosulfate reductase; SAT, ATP sulfurylase.

APS reductase (i.e., AprAB) and ATP sulfurylase (i.e., SAT) (Hensen *et al.*, 2006; Ghosh and Dam, 2009). Lastly, other bacteria oxidize reduced sulfur compounds via formation of a tetrathionate intermediate. These organisms have no *sox* genes or an incomplete set of *sox* genes (Ghosh and Dam, 2009). Environmental genomic data suggest that marine GSOs harbor incomplete sets of *sox* and *dsr* genes, oxidizing sulfur via the formation of a tetrathionate intermediate or via the branched thiosulfate oxidation pathway. This also suggests that they produce and store elemental sulfur in globules (Walsh *et al.*, 2009). The marine GSO isolate, *Thioglobus singularis* strain GSO-PS1, formed external sulfur globules when grown on seawater media (Marshall and Morris, 2013). This suggests that members of the Arctic96BD-19 subclade oxidize sulfur via the formation of a tetrathionate intermediate or via the branched thiosulfate oxidation pathway. Proteomic data provide further evidence suggesting that marine GSOs utilized the branched thiosulfate oxidation pathway (Figure 5).

In a previous study, critical genes for carbon fixation via the Calvin–Benson–Basham cycle (RuBisCO) were noted in the partial SUP05 metagenome, whereas genes for a complete tricarboxylic acid cycle, required for heterotrophic growth, were absent, suggesting that SUP05 GSOs are obligate chemolithoautotrophs (Walsh *et al.*, 2009). RuBisCO genes were also noted in partial Arctic96BD-19 genomes (Swan *et al.*, 2011). We observed marine GSO RuBisCO proteins in the Inferno vent plume, providing functional evidence that free-living marine GSOs fixed inorganic carbon. Iron oxidizers also contributed to primary production in the plume, as evidenced by the expression of an iron oxidizer RuBisCo (Supplementary Table 3).

Free-living members of the SUP05 subclade are known to thrive in low-oxygen waters (Walsh *et al.*, 2009; Zaikova *et al.*, 2010) and hydrothermal vent plumes (Sunamura *et al.*, 2004), whereas members of the Arctic96BD-19 GSO clade have been identified in oxygenated inshore and offshore waters, at hydrothermal vents and cold seeps and in the surface layer and deep ocean (Bano and Hollibaugh, 2002; Fuchs *et al.*, 2005; Murray and Grzymski, 2007; Kato *et al.*, 2009; Lavik *et al.*, 2009; Swan *et al.*, 2011). The Inferno hydrothermal vent plume was sufficiently oxygenated (dissolved oxygen ranged from 27.6 to 28.6 $\mu mol\,kg^{-1}$) for GSOs to respire aerobically, thus the discovery of COX subunits I and II provides direct evidence that aerobic respiration was employed (Figure 5). Much less is known about GSO sulfur oxidation in oxygenated waters throughout the deep ocean, where hydrogen sulfide is not present at high concentrations but less reduced forms of sulfur are available for further oxidation.

The presence of CH_4 oxidation proteins (pMMO) in the Inferno plume is consistent with the presence of both CH_4 and oxygen (Figure 3). The PmoA and PmoC polypeptides of pMMO were not observed. PmoA and PmoC are fully membrane bound, whereas PmoB has soluble domains (Lieberman and Rosenzweig, 2005). Membrane-bound peptides are difficult to extract and ionize due to their hydrophobic nature, reducing the chance of identification using a whole-cell MS/MS proteomic approach. However, we also identified a methanol dehydrogenase formaldehyde-activating enzyme (Fae) and putative methylotrophic transketolase that could participate in formaldehyde fixation via the ribulose monophosphate pathway (Trotsenko *et al.*, 1986). In combination, these data suggest that the

Inferno vent plume harbored type I methanotrophs that assimilated carbon from CH_4 using pMMO, methanol dehydrogenase and the ribulose monophosphate pathway (Figure 5).

It is clear from the organisms and enzymes identified in vent plumes that reduced compounds emitted from the deep subsurface have the potential to impact carbon cycling in the deep ocean when they mix with seawater and stimulate growth of a subset of free-living marine bacteria and archaea. Sulfur oxidizers, methylotrophs and iron oxidizers expressed key proteins associated with carbon fixation. Broader spatial and temporal studies of functions expressed in hydrothermal vent plumes will provide further insights into carbon cycling in the dark ocean and connectivity between the deep subsurface and deep ocean biospheres.

Conflict of Interest

The authors declare no conflict of interest.

Acknowledgements

We thank chief scientists J Delaney and D Kelley and officers and crew of the *R/V Thomas G Thompson*. This study was supported by grants from the National Science Foundation OCE-1232840 (RM Morris) and OCE-0825790 (BL Nunn) and National Institutes of Health 5P30ES007033-12 and 1S10RR023044. DAH was supported by OCE-1153930. TEM was supported by a University of Iowa Career Development Award.

References

Anantharaman K, Breier JA, Sheik CS, Dick GJ. (2013). Evidence for hydrogen oxidation and metabolic plasticity in widespread deep-sea sulfur-oxidizing bacteria. *Proc Natl Acad Sci USA* **110**: 330–335.

Anderson RE, Beltrán MT, Hallam SJ, Baross JA. (2013). Microbial community structure across fluid gradients in the Juan de Fuca Ridge hydrothermal system. *FEMS Microbiol Ecol* **83**: 324–339.

Baker ET, Massoth GJ, Walker SL, Embley RW. (1993). A method for quantitatively estimating diffuse and discrete hydrothermal discharge. *Earth Planet Sci Lett* **118**: 235–249.

Bano N, Hollibaugh JT. (2002). Phylogenetic composition of bacterioplankton assemblages from the Arctic Ocean. *Appl Environ Microbiol* **68**: 505–518.

Caress DW, Clague DA, Paduan JB, Martin JF, Dreyer BM, Chadwick WW *et al.* (2012). Repeat bathymetric surveys at 1-metre resolution of lava flows erupted at Axial Seamount in April 2011. *Nat Geosci* **5**: 483–488.

Cavanaugh CM, Levering PR, Maki JS, Mitchell R, Lidstrom ME. (1987). Symbiosis of methylotrophic bacteria and deep-sea mussels. *Nature* **325**: 346–348.

Chadwick WW, Nooner SL, Butterfield DA, Lilley MD. (2012). Seafloor deformation and forecasts of the April 2011 eruption at Axial Seamount. *Nat Geosci* **5**: 474–477.

Childress JJ, Fisher CR, Favuzzi JA, Sanders NK. (1991). Sulfide and carbon dioxide uptake by the hydrothermal vent clam, *Calyptogena magnifica*, and its chemoautotrophic symbionts. *Physiol Zool* **64**: 1444–1470.

Dick GJ, Tebo BM. (2010). Microbial diversity and biogeochemistry of the Guaymas Basin deep-sea hydrothermal plume. *Environ Microbiol* **12**: 1334–1347.

Dickson AG, Sabine CL, Christian JR (eds) (2007). *Guide to Best Practices for Ocean CO2 Measurements 191 pp.*

Distel DL, Lane DJ, Olsen GJ, Giovannoni SJ, Pace B, Pace NR *et al.* (1988). Sulfur-oxidizing bacterial endosymbionts: analysis of phylogeny and specificity by 16*S* rRNA sequences. *J Bacteriol* **170**: 2506–2510.

Dziak RP, Haxel JH, Bohnenstiehl DR, Chadwick WW, Nooner SL, Fowler MJ *et al.* (2012). Seismic precursors and magma ascent before the April 2011 eruption at Axial Seamount. *Nat Geosci* **5**: 478–482.

Eng JK, McCormack AL, Yates JR. (1994). An approach to correlate tandem mass spectral data of peptides with amino acid sequences in a protein database. *J Am Soc Mass Spectrom* **5**: 976–989.

Eng JK, Fischer B, Grossmann J, MacCoss MJ. (2008). A fast SEQUEST cross correlation algorithm. *J Proteome Res* **7**: 4598–4602.

Friedrich CG, Rother D, Bardischewsky F, Quentmeier A, Fischer J. (2001). Oxidation of reduced inorganic sulfur compounds by bacteria: emergence of a common mechanism? *Appl Environ Microbiol* **67**: 2873–2882.

Friedrich CG, Bardischewsky F, Rother D, Quentmeier A, Fischer J. (2005). Prokaryotic sulfur oxidation. *Curr Opin Microbiol* **8**: 253–259.

Fuchs BM, Woebken D, Zubkov MV, Burkill P, Amann R. (2005). Molecular identification of picoplankton populations in contrasting waters of the Arabian Sea. *Aquat Microb Ecol* **39**: 145–157.

Ghosh W, Dam B. (2009). Biochemistry and molecular biology of lithotrophic sulfur oxidation by taxonomically and ecologically diverse bacteria and archaea. *FEMS Microbiol Rev* **33**: 999–1043.

Hansell DA. (2005). Dissolved organic carbon reference material program. *EOS* **86**: 318.

Hensen D, Sperling D, Trüper HG, Brune DC, Dahl C. (2006). Thiosulphate oxidation in the phototrophic sulphur bacterium *Allochromatium vinosum*. *Mol Microbiol* **62**: 794–810.

Huang X, Madan A. (1999). CAP3: a DNA sequence assembly program. *Genome Res* **9**: 868–877.

Huber JA, Butterfield DA, Baross JA. (2003). Bacterial diversity in a subseafloor habitat following a deep-sea volcanic eruption. *FEMS Microbiol Ecol* **43**: 393–409.

Huber JA, Johnson HP, Butterfield DA, Baross JA. (2006). Microbial life in ridge flank crustal fluids. *Environ Microbiol* **8**: 88–99.

Huber JA, Mark Welch DB, Morrison HG, Huse SM, Neal PR, Butterfield DA *et al.* (2007). Microbial population structures in the deep marine biosphere. *Science* **318**: 97–100.

Iverson V, Morris RM, Frazar CD, Berthiaume CT, Morales RL, Armbrust EV. (2012). Untangling genomes from metagenomes: revealing an uncultured class of marine Euryarchaeota. *Science* **335**: 587–590.

Kato S, Hara K, Kasai H, Teramura T, Sunamura M, Ishibashi J-i *et al.* (2009). Spatial distribution, diversity and composition of bacterial communities in subseafloor fluids at a deep-sea hydrothermal field of the Suiyo Seamount. *Deep Sea Res Pt I* **56**: 1844–1855.

Lavik G, Stuhrmann T, Bruchert V, Van der Plas A, Mohrholz V, Lam P *et al.* (2009). Detoxification of sulphidic African shelf waters by blooming chemolithotrophs. *Nature* **457**: 581–584.

Lesniewski RA, Jain S, Anantharaman K, Schloss PD, Dick GJ. (2012). The metatranscriptome of a deep-sea hydrothermal plume is dominated by water column methanotrophs and lithotrophs. *ISME J* **6**: 2257–2268.

Lieberman RL, Rosenzweig AC. (2005). Crystal structure of a membrane-bound metalloenzyme that catalyses the biological oxidation of methane. *Nature* **434**: 177–182.

Lilley MD, de Angelis MA, Gordon LI. (1982). CH_4, H_2, CO and N_2O in submarine hydrothermal vent waters. *Nature* **300**: 48–50.

Lilley MD, Feely RA, Trefry JH. (1995). *Seafloor Hydrothermal Systems: Physical, Chemical, Biological, and Geological Interactions* vol. 91. AGU: Washington, DC.

Lupton JE, Delaney JR, Johnson HP, Tivey MK. (1985). Entrainment and vertical transport of deep-ocean water by buoyant hydrothermal plumes. *Nature* **316**: 621–623.

Marshall KT, Morris RM. (2013). Isolation of an aerobic sulfur oxidizer from the SUP05/Arctic96BD-19 clade. *ISME J* **7**: 452–455.

McCune B, Grace JB. (2002). *Analysis of Ecological Communities*. MjM Software Design: Gleneden Beach, OR.

Morris RM, Rappe MS, Connon SA, Vergin KL, Siebold WA, Carlson CA *et al.* (2002). SAR11 clade dominates ocean surface bacterioplankton communities. *Nature* **420**: 806–810.

Morris RM, Nunn BL, Frazar C, Goodlett DR, Ting YS, Rocap G. (2010). Comparative metaproteomics reveals ocean-scale shifts in microbial nutrient utilization and energy transduction. *ISME J* **4**: 673–685.

Morris RM, Frazar CD, Carlson CA. (2012). Basin-scale patterns in the abundance of SAR11 subclades, marine Actinobacteria (OM1), members of the Roseobacter clade and OCS116 in the South Atlantic. *Environ Microbiol* **14**: 1133–1144.

Murray AE, Grzymski JJ. (2007). Diversity and genomics of Antarctic marine micro-organisms. *Philos Trans R Soc Lond B Biol Sci* **362**: 2259–2271.

Opatkiewicz AD, Butterfield DA, Baross JA. (2009). Individual hydrothermal vents at Axial Seamount harbor distinct subseafloor microbial communities. *FEMS Microbiol Ecol* **70**: 413–424.

Panchaud A, Scherl A, Shaffer SA, von Haller PD, Kulasekara HD, Miller SI *et al.* (2009). Precursor ACquisition Independent From Ion Count: how to dive deeper into the proteomics ocean. *Anal Chem* **81**: 6481–6488.

Panchaud A, Jung S, Shaffer SA, Aitchison JD, Goodlett DR. (2011). Faster, quantitative, and accurate precursor acquisition independent from ion count. *Anal Chem* **83**: 2250–2257.

Proskurowski G, Lilley MD, Olson EJ. (2008). Stable isotopic evidence in support of active microbial methane cycling in low-temperature diffuse flow vents at 9°50′N East Pacific Rise. *Geochim Cosmochim Acta* **72**: 2005–2023.

Pruesse E, Quast C, Knittel K, Fuchs BM, Ludwig W, Peplies J *et al.* (2007). SILVA: a comprehensive online resource for quality checked and aligned ribosomal RNA sequence data compatible with ARB. *Nucleic Acids Res* **35**: 7188–7196.

Reinthaler T, van Aken HM, Herndl GJ. (2010). Major contribution of autotrophy to microbial carbon cycling in the deep North Atlantic's interior. *Deep Sea Res Pt II* **57**: 1572–1580.

Robinson JJ, Cavanaugh CM. (1995). Expression of form I and form II RuBisCo in chemoautotrophic symbioses: implications for the interpretation of stable carbon isotope values. *Limnol Oceanogr* **40**: 1496–1502.

Stothard P. (2000). The Sequence Manipulation Suite: JavaScript programs for analyzing and formatting protein and DNA sequences. *Biotechniques* **28**: 1102–1104.

Sunamura M, Higashi Y, Miyako C, Ishibashi J-i, Maruyama A. (2004). Two bacteria phylotypes are predominant in the Suiyo Seamount hydrothermal plume. *Appl Environ Microbiol* **70**: 1190–1198.

Swan BK, Martinez-Garcia M, Preston CM, Sczyrba A, Woyke T, Lamy D *et al.* (2011). Potential for chemolithoautotrophy among ubiquitous bacteria lineages in the dark ocean. *Science* **333**: 1296–1300.

Sylvan JB, Toner BM, Edwards KJ. (2012). Life and death of deep-sea vents: bacterial diversity and ecosystem succession on inactive hydrothermal sulfides. *MBio* **3**: 1–10.

Trotsenko YA, Doronina NV, Govorukhina NI. (1986). Metabolism of non-motile obligately methylotrophic bacteria. *FEMS Microbiol Lett* **33**: 293–297.

Walsh DA, Zaikova E, Howes CG, Song YC, Wright JJ, Tringe SG *et al.* (2009). Metagenome of a versatile chemolithoautotroph from expanding oceanic dead zones. *Science* **326**: 578–582.

Wang Q, Garrity GM, Tiedje JM, Cole JR. (2007). Naïve Bayesian classifier for rapid assignment of rRNA sequences into the new bacterial taxonomy. *Appl Environ Microbiol* **73**: 5261–5267.

Xie W, Wang F, Guo L, Chen Z, Sievert SM, Meng J *et al.* (2011). Comparative metagenomics of microbial communities inhabiting deep-sea hydrothermal vent chimneys with contrasting chemistries. *ISME J* **5**: 414–426.

Zaikova E, Walsh DA, Stilwell CP, Mohn WW, Tortell PD, Hallam SJ. (2010). Microbial community dynamics in a seasonally anoxic fjord: Saanich Inlet, British Columbia. *Environ Microbiol* **12**: 172–191.

Supplementary Information accompanies this paper on The ISME Journal website (http://www.nature.com/ismej)